Nonlinear Processes in Geophysics (2000) 7: 37–48

Nonlinear Processes in Geophysics

Searching for chaotic and deterministic features in laboratory water surface waves

M. Joelson[1], Th. Dudok de Wit[3], Ph. Dussouillez[2], and A. Ramamonjiarisoa[1]

[1]Laboratoire IRPHE-I0A, 163 Av. de Luminy, Marseille, France
[2]IRPHE Chateau Gombert, 38 Rue Frédéric Joliot Curie, Marseille, France
[3]LPCE-CNRS, 3A, Av. de la Recherche Scientifique, Orleans, France

Received: 15 December 1998 – Accepted: 8 December 1999

Abstract. The dynamic evolution of laboratory water surface waves has been studied within the framework of dynamical systems with the aim to identify stochastic or deterministic nonlinear features. Three different regimes are considered: pure wind waves, pure mechanical waves and mixed (wind and mechanical) waves. These three regimes show different dynamics. The results on wind waves do not clearly support the recently proposed idea that a deterministic Stokes-like component dominate the evolution of such waves; they are more appropriately described by a similarity-like approach that includes a random character. Cubic resonant interactions are clearly identified in pure mechanical waves using tricoherence functions. However, detailed aspects of the interactions do not fully agree with existing theoretical models. Finally, a deterministic motion is observed in mixed waves, which therefore are best described by a low dimensional nonlinear deterministic process.

1 Introduction

The water surface waves motions are known to exhibit more or less strong irregularities. From the fundamental as well as practical viewpoint, three types of wavefields are of particular interest: *i.)* pure wind generated waves, *ii.)* swell and *iii.)* swell under wind action. For many years, the irregularities in these fields have been at least implicitly attributed to different causes. In wind generated waves, they were often attributed to the random character of the motion, owing to the turbulent nature of the wind flow. Then, probabilistic analysis of these waves have been carried out (see e.g. Phillips, 1977). On the other hand, their nonlinear features being now recognized, they would be seen as nonlinear oscillations driven by a stochastic force and, then, classified as nonlinear stochastic dynamical systems. However, the few analytical developments made in that direction (West, 1982; Middleton and Mellen, 1985), apparently, did not attract the specialized scientific community attention. Instead, the discovery of the dispersionless nature of wind waves (Ramamonjiarisoa, 1974) yielded to propose that the evolution of such waves is dominated by a deterministic Stokes-like component. Then, the observed irregularities, rather than due to the randomness would be attributed to the instabilities of this dominant. These instabilities are now considerably documented (see Yuen and Lake, 1980). According to such proposition wind waves and nonlinear swells share common basic dynamics, of deterministic character. In a logical way, a mixed wavefield (swell under wind action) would also share such dynamics.

In the past, the irregularities of surface wavefields were characterized through an extensive use of the spectral analysis. Undoubtedly, this yielded to fundamental progress in the understanding of the physical processes involved in the wave evolution. Most of the above results were obtained through spectral analysis. However, such analysis is known to be insufficient to make clear distinction among stochastic, deterministic, combined stochastic and deterministic behaviours especially for the situations which will be examined herein which proved to be typical of laboratory wavefields evolution.

Recently, new methods for characterizing irregular behaviour have been developped in the framework of the so-called nonlinear dynamical system. They have been widely applied with success to various systems (see e.g. Summhammer et al, 1987; Tsonis and Elsner, 1990; Buzug et al, 1992; Herzel et al, 1994;...). In principle, they are able to make distinction between the above three behaviours. Few applications to water surface waves and connected technical fields exist this time. But they appear to be not much conclusive. Some of the methods are used here, in addition to the classical spectral analysis, to explore data obtained from laboratory

Correspondence to: M. Joelson

experiments with two main objectives in mind. The first objective deals with looking at more experimental evidence of nonlinear evolution in wavefield. The second objective is concerned with the identification, if possible, of the nature of the various observed wave motions. This would help, in particular, to confirm or to refute some of the above proposed physical models of evolution.
The experiments are briefly presented in § 2. In § 3, the analysis methods are described with a first comments concerning their significance from the physical viewpoints. Then, the main results are reported (§ 4) and discussed on physical grounds (§ 5). The main conclusions are briefly recalled in § 6.

2 The experiments

The data of interest issue from experiments made in the wind wave facility of the IRPHE-IOA Laboratory. Basically, the facility consists of a water tank of 40 m length, 3 m width and 1 m depth. An air flow, with velocities ranging from 0 m/s to about 15 m/s generates wind wave fields. In addition, the facility is equipped with an electro-hydraulic wave maker producing swells with frequencies ranging from about 1 to 2 Hz. Various types of surface waves can be produced by separated or by combined action of the air flow and the wave maker.

It is to be stressed that the facility includes particular devices intended to control various parasitical effects which could coexist with the physical process under consideration. In particular, a permeable wave absorber is disposed at the upwind end of the water tank to prevent the wave reflection. Within the range of wave frequency of interest in the experiments on surface waves, the reflection coefficient is estimated to be less than 5%. As far as wind generated waves are concerned, a specific design has been adopted for a smooth joining of the air flow and the water surface. The design prevents air flow separation at the facility entrance test section. This insures a natural development of the turbulent boundary layer over the water surface. In addition, later quays disposed in the water tank favor the three-dimensional evolution of the wind waves. Studies with more details about there specific devices are given in a number of publications (see e.g. Ramamonjiarisoa, 1974; Coantic and Favre, 1974).
We concentrate here on the time evolution of the water surface deflection level at a given position. The recordings were made using a capacitance wire gauge of 0.3 mm outer diameter; the capacity of this gauge varies linearly with the surface deflection level; the sensitivity of the device is about 0.6 V/cm, giving a resolution of the order of 0.1 mm.

Experiments were carried out under various conditions, whose main parameters are the wind velocity, the amplitude and the frequency of the wave maker, and the distance between the gauge and the wave maker (hereafter denoted fetch). In which follows, we consider three particular runs that are indicative of the different types of behaviour observed:

1. waves generated by wind only (velocity 10 m/s)
2. waves generated by wave maker only (frequency 1.7 Hz, wave steepness 0.25)
3. waves generated by wind (velocity 10 m/s) and wave maker (frequency 1.2 Hz, initial wave steepness 0.15)

In each run, the gauge was fixed at 35 m from the wave maker. Then, the waves had sufficiently long space to evolve dynamically.
The choice of the above conditions was dictated by the following arguments:
a.) well developed pure wind generated laboratory gravity waves fields are known to exhibit similar statistical properties whatever the fetch and the wind velocity may be. The similarity is seen in the spectral density functions, the probability density function as well as in the dispersion relation (see Ramamonjiarisoa, 1973; Toba, 1973) . Of particular interest is that the so-called significant wave steepness is of the order of 0.25. The particular condition corresponds to a dominant wave frequency of about 1.5 HZ which is close to the frequency of the pure mechanically generated wavefield. In addition, the actual wind wavefield possesses sufficiently high amplitude which favours accurate measurements and determination of the various quantities of interest in the study.
b.) the pure mechanical waves have an initial wave steepness of 0.25, close to the significant wave steepness of the pure wind waves. The analyzed signal corresponds to the largest fetch available. As seen in Figure 1 in this location, the field has reached a chaotic state, which strongly differs from the regular motion (not reported here), observed at shorter fetch associated with the Benjamin-Feir instability. We are interested here in the long term behaviour of the wavefield. The short term behaviour has been already the subject of several investigations by many authors.
c.) In the mixed field, the initial wave steepness of the mechanical wave is 0.15. Due to the amplification by the wind, the steepness increases along the fetch so that the field will become more and more nonlinear. At the point of measurement, the steepness is estimated to be of order 0.26. The wind velocity is chosen sufficiently high so that to be eventually able to perturb the regular behaviour of the mechanical wave. The combination of the wave nonlinearity and the wind action was expected to produce a stochastic evolution. Surprisingly, as will be shown, this appears to be not the case.
As said previously, only time variations of the water surface defection level at given locations in space are available from the measurements. The corresponding

processed series are made of $n = 72115$ samples gathered at a continuous rate of 200 Hz. Generally speaking, the water surface wavefields of interest here are known to have temporal as well as spatial dynamics in which dispersion, nonlinearity, dissipation (by the kinematic viscosity or by breaking) and eventually wind action are involved. The results presented herein are limited to some aspects of the temporal evolution at the given space locations. In such case, the dispersion effect was found to be quite negligible. Then, the work is intended to give insight on the rôle of the others cited processes, especially, as far as the chaotic or deterministic features of the fields are concerned.
It is to be stressed again that many others runs have been conducted under various experimental conditions but no results which significantly differ from those reported here have been found.

3 Analysis methods

In this section we present four different analysis methods that were applied to the data, in addition to classical spectral and statistical methods. The experimental analysis of deterministic nonlinear systems is nowadays receiving growing interest (Tsonis, 1992; Ott et al., 1994, Abarbanel, 1996; Kantz and Schreiber, 1997) but only few studies have been devoted to water waves (Mayer-Kress and Elgar, 1989; Haykin and Puthusserypady, 1997). That these do not adequately fit into the categories of deterministic or stochastic systems, may explain the problems encountered in describing them.

3.1 Phase space analysis

One of the simplest and yet powerful methods for getting qualitative information from a physical process is by exploring its phase space. Most experiments, however, do not give direct access to the phase space or are too noise-dominated to enable the computation of higher order derivatives. Time-delay embedding often provides a satisfactory alternative to this problem (Kantz and Schreiber, 1997). Given a single scalar measurement, it allows us to reconstruct a phase space that, under mild conditions, is topologically equivalent to the true one. Consider the regularly sampled water level measurements $[\eta(t_1), \eta(t_2), \ldots, \eta(t_n)]$, then the ensemble of points whose coordinates are

$$X(t) = (\eta(t), \eta(t-\tau), \eta(t-2\tau), \ldots, \eta(t-(m-1)\tau)) \quad (1)$$

defines an orbit in m-dimensional phase space. The time evolution of the system is then depicted qualitatively by the way the orbits move away the points $X(t)$. Such orbits provide the basis for the various analysis methods that have been developed in the framework of dynamical systems (Eckmann and Ruelle, 1985).

Once the orbits are reconstructed by time-delay embedding, it is often desirable to have a reference set to which the data can be compared. A classical test involves surrogate data: a time series is generated, which mimics the properties of the observations (having the same power spectral density and the same probability density) but in which signatures of nonlinearity, i.e. deterministic phase couplings between Fourier modes, are destroyed. A simple way of doing this is by computing the Fourier transform, randomizing the phases and then performing the inverse transform (Theiler et al., 1992). We can thereby test the hypothesis whether the data are the output of a linear system driven by stochastic forces (and possibly transformed by a static nonlinear filter).

The main problem here is the choice of the time lag τ (which is necessarily a multiple of the sampling period) and the embedding dimension m. There exist various criteria for selecting the embedding dimension (Abarbanel, 1996; Kantz and Schreiber, 1997). As far as we merely want to have a qualitative look at the phase space, we shall be content here with a relatively small value $m = 2$. More important is the choice of the time lag τ, for which there also exist various selection criteria. The lag should be such that the two time series $\eta(t)$ and $\eta(t-\tau)$ are reasonably decorrelated. An obvious choice would then be to take the smallest time lag τ for which the autocorrelation function $R_{\eta\eta}(\tau) = \langle \eta(t)\eta(t+\tau) \rangle$ (where brackets denote ensemble averaging) vanishes or becomes small enough. It is generally agreed upon, however, that the mutual information approach, to be described now, is more adequate for such purposes.

3.2 Mutual information at different lags

Let η and μ be two random variables whose probability densities are respectively $P_\eta(\eta)$ and $P_\mu(\mu)$. The informational content of these variables is known to be associated with their entropies $H_\eta = -\int P_\eta(\eta) \log P_\eta(\eta) d\eta$ and $H_\mu = -\int P_\mu(\mu) \log P_\mu(\mu) d\mu$; the joint entropy is $H_{\eta\mu} = -\int P_{\eta\mu}(\eta, \mu) \log P_{\eta\mu}(\eta, \mu) d\eta d\mu$. The mutual information between the two variables, defined as

$$J_{\eta\mu} = H_\eta + H_\mu - H_{\eta\mu} \ , \quad (2)$$

tells us how much information we gain about one of the two processes given knowledge of the other (Fraser and Swinney, 1986). This mutual information vanishes if and only if the two processes are independent, that is if $P_{\eta\mu}(\eta, \mu) = P_\eta(\eta) P_\mu(\mu)$. The mutual information in this sense provides a more global measure of independence.

Here, the random variables η and μ are respectively the water level and the same time series delayed by τ. The mutual information thus becomes a function of the time lag, which we shall write as $I(\tau) = J_{\eta(t)\eta(t-\tau)}$. Notice that the empirical probability densities are discrete and so in practice the integrals in the definition are replaced by summations over different bins.

The optimum time lag τ for reconstructing the phase space is frequently chosen to be the value that gives the first local minimum of $I(\tau)$ (Fraser and Swinney, 1986). In most applications the mutual information is indeed restricted to that single use, although it obviously contains more pertinent information. In particular, a comparison between values of the mutual correlation, as computed for real and for surrogate data, should reveal whether nonlinearity generates correlations that would go undetected by standard linear correlation analysis.

3.3 Dimension analysis

Dimension calculations have become a standard method for quantifying low-order determinism in dissipative systems (Eckmann and Ruelle, 1985; Abarbanel, 1996; Kantz and Schreiber, 1997). Best known is the correlation dimension which, loosely speaking, reveals the effective number of degrees of freedom associated with the system. A finite dimension is associated with the existence in phase space of an attractor, whose shape can actually be highly intricate. Our system being spatially extended, there is a priori no reason for such a finite dimension to exist.

The estimation of correlation dimensions from embedded phase spaces has nowadays become a standard although certainly not a trivial procedure. First, the correlation integral is estimated

$$c_m(r) = \lim_{n\to\infty} \frac{1}{n(n-1)} \sum_{i,j=1,i\neq j}^{n} H(r-||X(t_i)-X(t_j)||) \ , \quad (3)$$

where $H(.)$ is the Heaviside function and the norm $||.||$ can be Euclidian or a different one. The correlation integral should in principle scale with the radius r of the hyperballs in m-dimensional phase space like

$$\lim_{r\to 0} c_m(r) \propto r^{\nu} \ , \quad (4)$$

The exponent ν is estimated for increasing values of m; if the system has a low-dimensional attractor, then ν should converge toward the correlation dimension provided that $m > 2\nu$. We must stress that finite sample size effects and the omnipresence of noise severely restrict the access to small radii r and large dimensions m, and hence to high dimensions. In our case, dimensions typically in excess of 4 cannot be meaningfully assessed.

3.4 Nonlinear wave interactions

A complementary and in some sense more natural description of nonlinear water waves issues from models of weakly interacting waves. Such models have received much attention in the past (Vyshkind and Rabinovich, 1976), and have been extensively studied in the framework of Hamiltonian systems (Zakharov et al., 1985). It is well established that nonlinear wave-wave interactions do occur between waves provided the resonance conditions:

$$f_1(\mathbf{k}_1) + f_2(\mathbf{k}_2) = f(\mathbf{k}_1 + \mathbf{k}_2) \ , \quad (5)$$

for three-wave interactions and

$$\begin{aligned} f_1(\mathbf{k}_1) + f_2(\mathbf{k}_2) + f_3(\mathbf{k}_3) &= f(\mathbf{k}_1 + \mathbf{k}_2 + \mathbf{k}_3) \quad (6) \\ f_1(\mathbf{k}_1) + f_2(\mathbf{k}_2) &= f_3(\mathbf{k}_3) + f(\mathbf{k}_1 + \mathbf{k}_2 + \mathbf{k}_3) \ , \end{aligned}$$

for four-wave interactions are satisfied. Here f is the frequency and $\mathbf{k}$ the wave number. Three-wave interactions can be ascribed to nonlinearities of the quadratic type. Their characteristic signature is an asymmetry of the probability density (Kim and Powers, 1979). Four-wave interactions are associated with nonlinearities of the cubic type. Typical examples are decay instabilities for the former, and modulational instabilities for the latter. The appropriate quantities for assessing the strength of three- and four-wave interactions are respectively the bispectrum and the trispectrum (Subba Rao and Gabr, 1984; Nikias and Petropulu, 1993). Both are direct generalizations of the power spectral density to multipoint correlations. The bispectrum reads

$$B(f_1, f_2) = \langle \tilde{\eta}(f_1)\tilde{\eta}(f_2)\tilde{\eta}^*(f_1 + f_2)\rangle \ , \quad (7)$$

and the trispectrum

$$T(f_1, f_2, f_3) = \langle \tilde{\eta}(f_1)\tilde{\eta}(f_2)\tilde{\eta}(f_3)\tilde{\eta}^*(f_1 + f_2 + f_3)\rangle \ , \quad (8)$$

where $\tilde{\eta}(f)$ is the Fourier transform of the time series $\eta(t)$, the superscript * denotes complex conjugation and brackets denote ensemble averaging.

Nonzero values of these higher order spectra arise only when deterministic phase couplings exist between Fourier modes whose frequencies satisfy the resonance conditions (Eqs. 5 and 6). Such phase couplings are a necessary (but not always sufficient) condition for having nonlinear wave interactions.

In practice, it is more convenient to normalize higher order spectra in order to have a quantity that is bounded between 0 and 1. The normalized bispectrum is called the bicoherence

$$b^2(f_1, f_2) = \frac{|B(f_1, f_2)|^2}{\langle |\tilde{\eta}(f_1)\tilde{\eta}(f_2)|^2 \ |\tilde{\eta}^*(f_1 + f_2)|^2\rangle} \ , \quad (9)$$

and the normalized trispectrum the tricoherence

$$t^2(f_1, f_2, f_3) = \frac{|T(f_1, f_2, f_3)|^2}{\langle |\tilde{\eta}(f_1)\tilde{\eta}(f_2)\tilde{\eta}(f_3)|^2 |\tilde{\eta}^*(f_1 + f_2 + f_3)|^2\rangle} \quad (10)$$

Both quantities have become standard indicators for nonlinearity and non-Gaussianity in time series (Nikias and Petropulu, 1993, and references therein). We just mention that there exist other, slightly different variants in their definition (Kravtchenko-Berejnoi et al., 1995).

4 Results

We now go through the results obtained using the various analysis methods, starting with the classical ones. A synthesis follows in the next section.

4.1 Spectra and probability density function

Figure 1 summarizes the basic properties of the wavefield, with an excerpt of the time series, the probability density and the power spectral density. The three runs correspond to wind waves (*i.*), pure mechanical waves (*ii.*), and mixed waves (*iii.*).

A first striking result is the large amplitude and high coherence of the waves obtained by combined action of wind and wave maker (*iii.*) as compared to waves generated solely by wind or by wave maker. The random-like character of the latter is attested by probability densities that are close to Gaussian, whereas in case (*iii.*) the density is more akin to that of a sinusoidal wave embedded in random noise (see e.g. Middleton, 1960). The asymmetry of the probability density further suggests that the waves are rather of the Stokes type than sinusoidal. Such an asymmetry is a typical signature of quadratic wave interactions, which will be evidenced below by the bicoherence analysis.

An inspection of the power spectral densities reveals further differences between the three cases. The energy level around the peaks are quite different. This could raise question about the validity of the comparison of the three runs. This has been discussed in section 2 considering the respective values of the significant wave steepness which is generally accepted as indicative of the nonlinearity level of the wavefields. The aperiodic structure of wind waves (*i.*) is evidenced by a broad maximum in the power spectral density. Pure mechanical waves on the other hand show several spectral lines, one of which occurs at the wavemaker frequency. At the actual stage of the fetch evolution, the presence of such a discrete spectrum is reminiscent of the modulational instability, which has been well documented in laboratory experiments (Benjamin and Feir, 1967). We note the occurrence of a "frequency downshift" since the most energetic spectral line is not the one associated with the carrier at $f = 1.7$ Hz (as observed for smaller fetches) but its lower sideband. It is known that such an asymmetric development of sidebands cannot be predicted by classical instability theory.

The power spectral density of mixed waves (*iii.*) is also highly peaked at the wave maker frequency but shows no evidence for subharmonic transitions; we observe instead a single fundamental with its harmonics. This already suggests that the random forcing of the wind prevents the modulational instability from developing like in case (*ii.*).

We note that at high frequencies the power spectral density of wind generated waves exhibits a power-law decay $P(f) \propto f^{\gamma}$ (γ is estimated in order of $-\frac{7}{3}$ for wind waves). The existence of such a scaling is a well-known feature of self-similar processes (see e.g. Kitaigorodskii, 1987). The present work focuses on the frequency band surrounding the frequency of the fundamental mode. Therefore, smaller scales, which are of interest the study of wind-wave interactions, will not be considered.

4.2 Autocorrelation and mutual information functions

The autocorrelation function and the mutual information are compared in Figure 2. We estimated the mutual information using a grid of 10 equiprobable intervals (see Fraser and Swinney, 1986) but the results are qualitatively identical for other numbers of bins. As a measure of uncertainty, we take the bias of this empirical estimate, which is calculated to be about 0.01 bit.

Both the autocorrelation function and the mutual information reveal oscillations that are characteristic of a narrow band process. Recall that the optimum time lag τ for reconstructing the phase space by delay embedding is given either by the first zero of the autocorrelation function (giving τ_{corr}) or by the first minimum of the mutual information (giving τ_{mut}). The following values of τ_{mut} and τ_{corr} are found (with an uncertainty of typically 0.02 sec.)

case	τ_{mut} [sec]	τ_{corr} [sec]
i.)	0.175	0.17
ii.)	0.145	0.16
iii.)	0.195	0.215

The closeness of the values, as estimated by the two methods, suggests that the nonlinearity is rather weak in all three cases. To evidence the effect of nonlinearity, we compare the values of the mutual information as computed from real and from surrogate data, see Figure 2. We recall that the surrogate data have the same properties as the original data, but without signatures of nonlinearity. In case (*i.*) the difference is barely significant and so n nonlinearity does not have to be invoked per se to explain the wavefield dynamics. A greater discrepancy appears in cases (*ii.*) and (*iii.*) where evidence is found for a deterministic phase coupling between Fourier modes. At this stage we may conclude that the the nonlinearity increases the degree of coherence of the wavefield. In (*ii.*) this enhancement mainly concerns adjacent crests of the fundamental oscillation whereas in (*iii.*) the effect extends over many periods. Such an effect should be visible in the phase portraits, to be examined now.

4.3 Phase portraits

Since we know the optimum time lag τ, we can attempt a partial reconstruction of the phase space by delay embedding. As mentioned before, we restrict ourselves

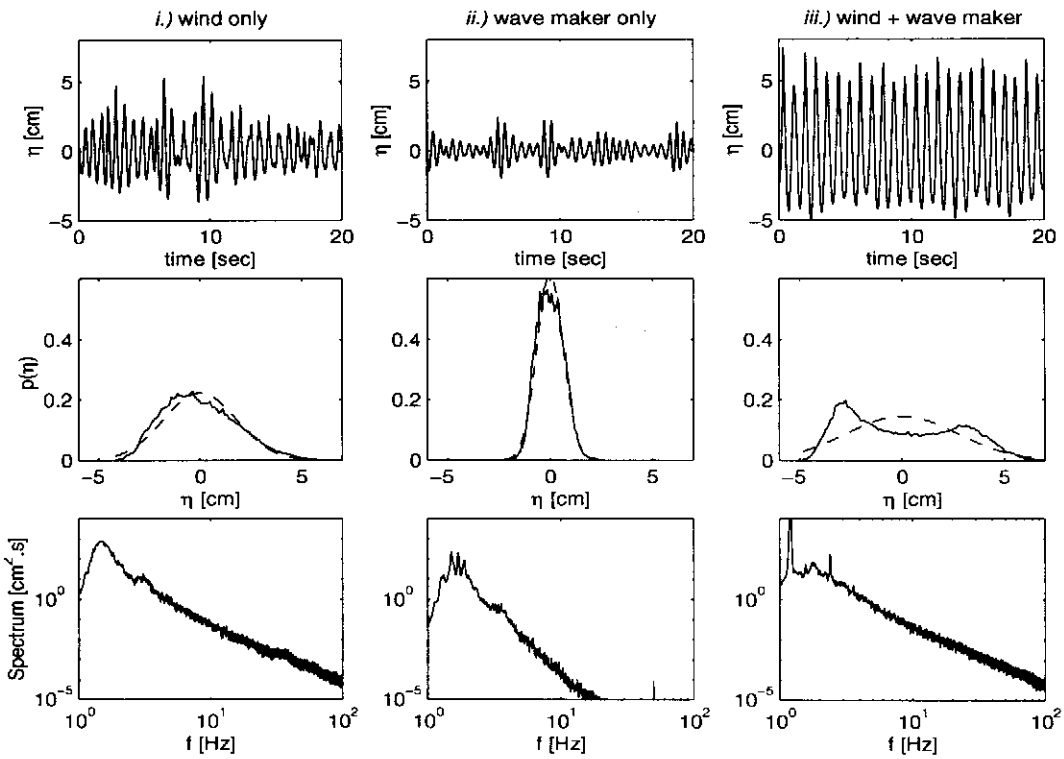

Fig. 1. Key properties of wind-generated waves, with from top to bottom: an excerpt of time evolution of the water deflection level (units are centimeters); the probability density of the wavefield (dashed lines corresponds to a Gaussian density of the same variance and zero mean); power spectral density on a logarithmic scale. The three columns respectively correspond to wind waves, pure mechanical waves and mixed waves.

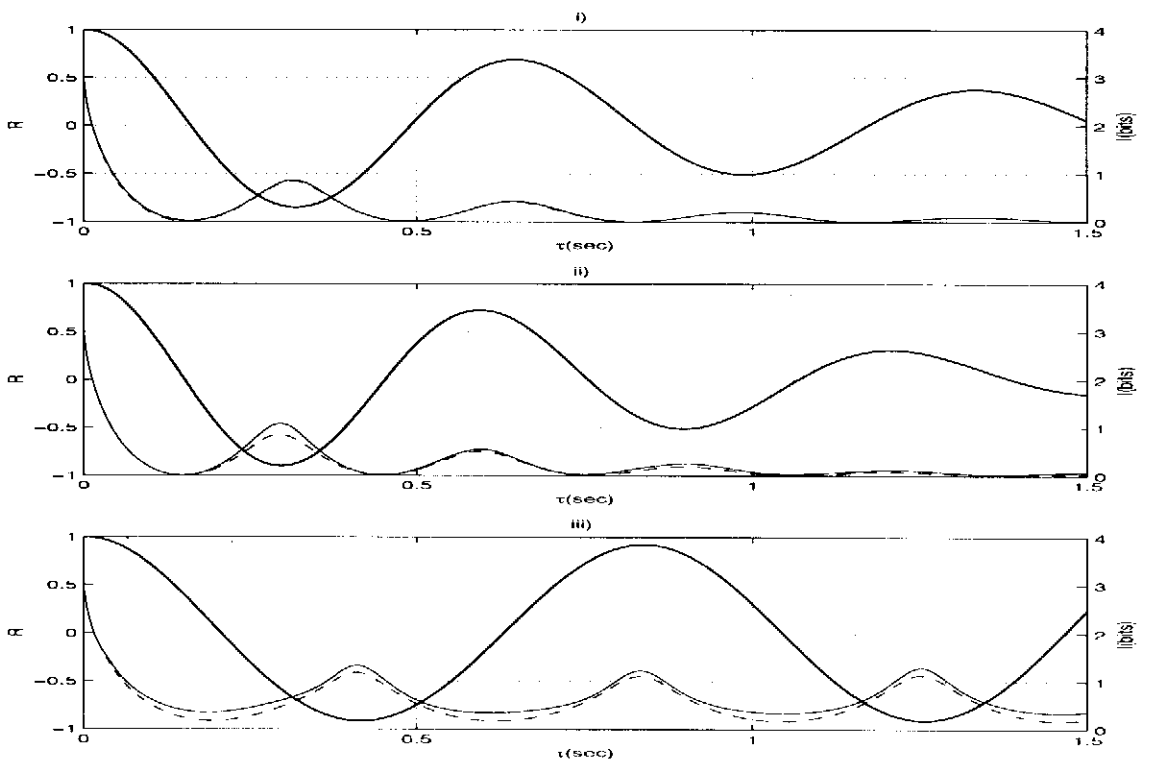

Fig. 2. Autocorrelation (thick line) and mutual information as computed for cases (*i.*)-(*iii.*). Also shown is the mutual information computed from surrogate data (dashed line), in which signatures of nonlinearity are destroyed.

here to two-dimensional projections of the phase space, whose true dimension is not known a priori. Figure 3 shows the reconstructed phase portraits.

All three phase portraits have in common a dominant cyclic feature, but their fine structure reveals marked differences. Wind generated waves (*i.*) show the most erratic behaviour, with wiggles indicating that there is no clear connection between low and high frequencies (as compared to the frequency of the fundamental).

A stronger coupling between Fourier modes is evident in pure mechanical waves (*ii.*) since, even though the power spectral density is comparable to that of (*i.*), the high frequency distortions are not distributed throughout the phase space anymore but arise in a more ordered way. Surprisingly, it is the combined action of wind and wave maker that yields the most structured phase portrait, see Figure 3. Indeed, the trajectories concentrate on well structured orbits (an "attractor") that are the hallmark of determinism. Given the sensitivity of the probes and the experimental conditions, we cannot attribute the thickness of the attractor to experimental noise. It thus remains to be determined whether the observed attractor has a fine structure or if it width just results from the stochastic action of the wind and dissipation. To answer this question, we now investigate the correlation dimension.

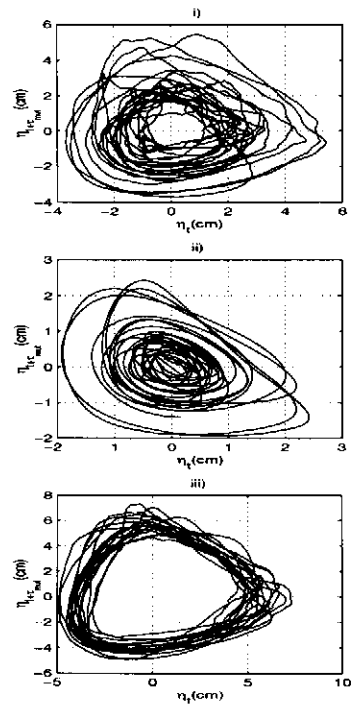

Fig. 3. Two dimensional phase portraits as reconstructed from the three time series by delay embedding. The time lags τ_{mut} are set by the first minimum of the mutual information: $\tau_{mut} = 0.175$ sec (*i.*), $\tau_{mut} = 0.145$ sec (*ii.*), and $\tau_{mut} = 0.195$ sec (*iii.*).

4.4 Correlation dimensions

The dimension analysis of the wavefield is summarized in Figure 4, in which the logarithmic derivative of the correlation integral $d \log c_m(r)/d \log r$ is displayed vs the size r of the hyperballs in phase space. Time lags computed by mutual information were used to reconstruct embedded phase spaces of dimensions ranging from $m =$ 1 to 10.

If Eq. (4) holds, then the curves in Figure 4 should all flatten and saturate for large m; the level of the plateau then corresponds to the correlation dimension of interest. We must stress that the limited sensitivity of the probes prohibits access to structures whose size is smaller than $r < 10^{-3}$ which correspond to water level fluctuation less than 0.5mm. Figure 4 shows that there is no evidence for a saturation of the correlation integral with either wind or pure mechanical waves. We conclude that the wavefield dimension is either infinite or too large (typically larger than 4) to be quantified. A finer analysis of the saturation and a comparison with surrogate data suggest that such a dimension, if it exists, is likely to be smaller for mechanical than for wind waves.

The situation is again quite different for mixed waves (*iii.*), since the onset of a plateau is observed, clearly attesting the presence of a low dimensional attractor. The measured dimension is $D_2 = 1.3 \pm 0.05$, a value that is indeed compatible the type of limit cycle observed in Figure 3. The noninteger value of the dimension indi-

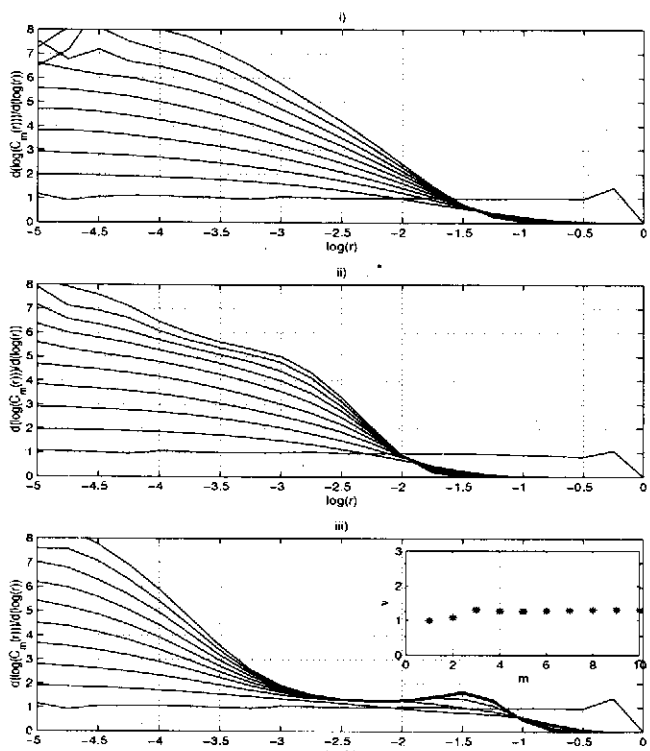

Fig. 4. Logarithmic derivative of the correlation integrals, as computed from the three time series, with different dimensions m and different sizes r of the hyperballs. Time lags obtained by mutual information criteria were used to reconstruct the phase spaces, but the results are relatively robust against the exact value of the lags.

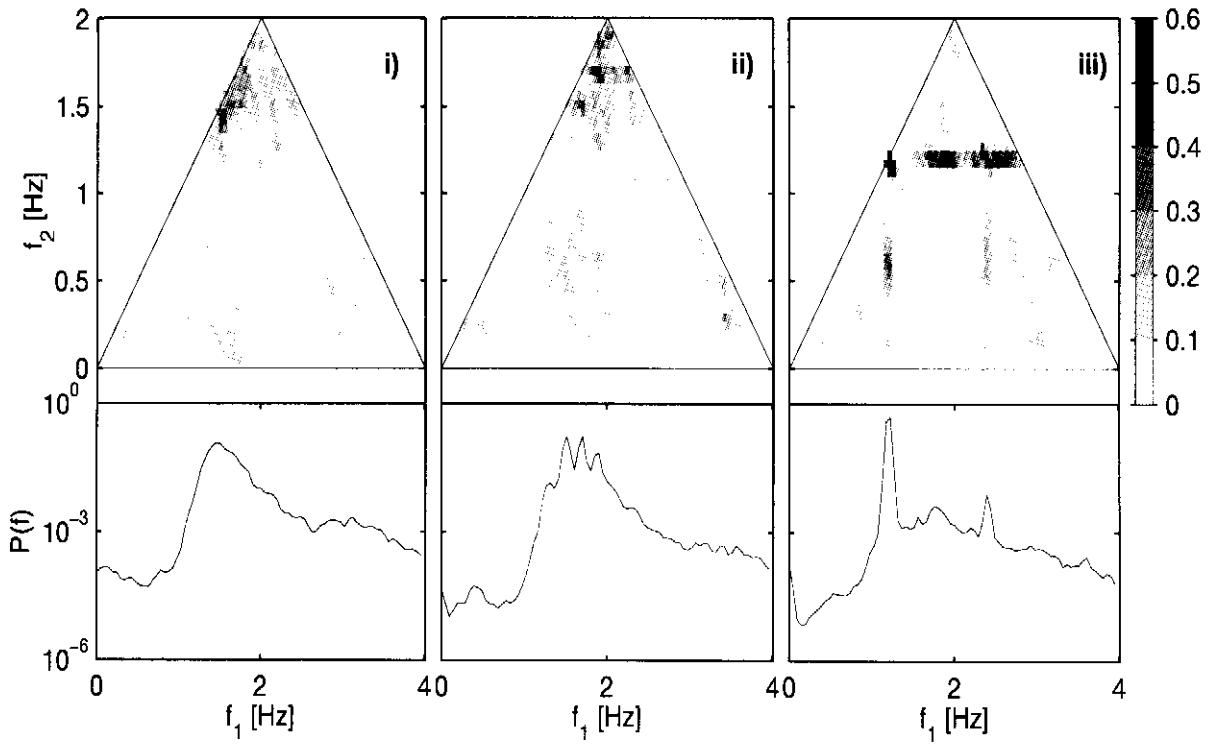

Fig. 5. Bicoherence as estimated for the three data sets. The display is restricted to the principal domain, which is bordered by a line. For the sake of clarity, the corresponding power spectral densities are also shown on the same plots. Since the empirical bicoherence estimator is biased, values below 0.2 are not considered to be significant.

cates that we have a *strange* attractor, whose topology is intermediate between a limit cycle and a torus. Such strange attractors are a typical feature of deterministic chaos in dissipative systems. We may therefore conclude that the highly regular waveform, and its small modulation, have their origin deeply rooted into the nonlinear nature of the process we consider. The surprise comes from the fact the presence of a stochastic forcing (the wind) and a deterministic forcing (the wave maker) can yield to a such a low dimensional dynamics since the same forcings, taken independently, lead to more complex behaviour as far as the dimensionality is concerned. Dissipations processes are necessarily present to generate a strange attractor. It is likely that incipient breaking of wave crests, as visually seen during the experiments, constitute the dominant process. Unfortunately, this process is far from being understood and still constitute one of the main problems which concern the nonlinear evolution of water waves. As suggested by the referee of the present work, the clear ridge of quadratic phase coupling on fig.5 could be indicative of the presence of such nonlinear dissipative mechanism.

4.5 Nonlinear Wave Interactions

Let us now consider the observations in terms of weakly interaction Fourier modes, and for that purpose compute higher order spectra. Figures 5 and 6 respectively show the bicoherence and the tricoherence functions, which quantify the strength of three- and four-wave interactions. The results were obtained by decomposing the time series into 35 partially overlapping blocks of 4096 samples, computing the Fourier transform for each of them, and subsequently averaging over the different blocks.

Because of the real-valued nature of the data, the bi- and tricoherence do not have to be estimated for all possible combinations of frequencies (see for example Nam and Powers, 1994). Here, we restrict ourselves to the non-redundant fraction of the frequency domain, whose limits are indicated by lines in Figures 5 and 6. The principal domain is a triangle for the bicoherence and a tetrahedron for the tricoherence.

4.5.1 Bicoherence

The bicoherence is depicted in Figure 5 for the three runs. For wind-generated waves ($i.$), we measure a small bicoherence except for frequencies that approximately satisfy the summation rule $1.4 + 1.4 = 2.8$ Hz. The maximum bicoherence is $b^2 = 0.4$, to be compared with unity for triads of waves that are fully phase coupled to each other. The interpretation of this maximum is relatively simple: the resonant frequency $f = 1.4$ Hz correponds to the peak in the power spectral density, so we are dealing with a self-interaction of the fundamen-

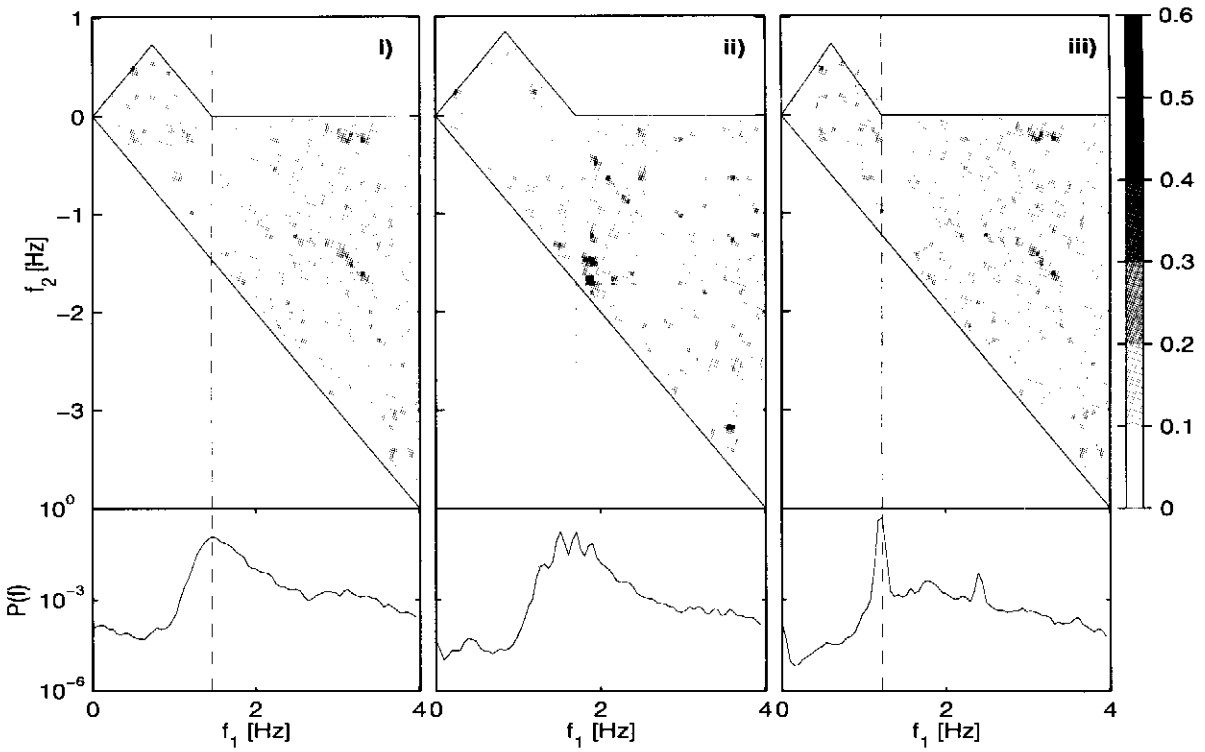

Fig. 6. Tricoherence as estimated the three data sets. The display is restricted to the principal domain, which is bordered by a line. The reference frequencies (shown by a dashed line) are from left to right $f_0 = 1.4$ Hz, $f_0 = 1.69$ Hz, and $f_0 = 1.2$ Hz. For the sake of clarity, the corresponding power spectral densities are also shown on the same plots. Since the empirical tricoherence estimator is biased, values below 0.2 are not considered to be significant.

tal, giving a first harmonic at $f = 2.8$ Hz. This is a typical feature of Stokes waves.

The same harmonic generation is observed for pure mechanical waves (*ii.*). The maximum value of the bicoherence is now slightly larger, possibly because the sharpness of the spectral lines makes the couplings more efficient. Harmonic generation is even stronger for mixed waves (*iii.*), with a bicoherence reaching $b^2 = 0.6$ for the self-interaction of the carrier $1.2 + 1.2 = 2.4$ Hz. Notice the existence also of an interaction between the fundamental and its first harmonic $1.2+2.4 = 3.6$ Hz. Interactions with higher harmonics are observed when extending the frequency range of the display. These results are in agreement with the asymmetric shape of the probability density, see Figure 1. A novel feature, however, is the broadband coupling we observe between the fundamental and higher frequency modes. This coupling, which is evidenced by the ridge ($f_1 > 1.2, f_2 = 1.2$) Hz, indicates that high frequency waves are enslaved to the fundamental. We had already conjectured such a coupling when considering the structured shape of the phase portraits, but the bicoherence now gives direct evidence for it. This coupling is easily understood if we remember that the wind-generated wavelets always occur at the crest and not at the bottom of the waves. The causal relationship between the carrier and the high frequency waves then manifests itself as a phase coupling.

4.5.2 Tricoherence

Since the tricoherence $t^2(f_1, f_2, f_3)$ is uneasy to visualize, we fix one of its frequencies and display the results in two dimensions. A suitable choice of the reference frequency often suffices to capture most of the pertinent information. A natural choice is to take the carrier frequency (*iii.*) or the frequency of the dominant mode (*i.*), and (*ii.*). The reference frequency is shown by a dashed line in Fig. 6. Concerning the interpretation of the tricoherence, we note that the upper triangle ($f_1 > 0, f_2 > 0$) corresponds to interactions of the type $f_1 + f_2 + f_3 = f_0$, with $f_0, f_1, f_2, f_3 > 0$. The lower triangle ($f_1 > 0, f_2 < 0$) corresponds to interactions of the type $f_1 + f_3 = f_0 + f_2$ or $f_1 = f_0 + f_2 + f_3$, again both with $f_0, f_1, f_2, f_3 > 0$.

For wind waves (*i.*), the measured tricoherence level is not significant and so we conclude that there is no clear evidence for four wave interactions. Previous investigations of wind waves (see e.g. Deardorff, 1967) indeed suggest that the corresponding spectral energy distribution should rather conform to the similarity theory. The same result holds for mixed waves (*iii.*), where the tricoherence is also negligible.

Pure mechanical waves, on the contrary, show significant couplings between the carrier and its sidebands. Different types of interactions can be found, depending

on the choice of the reference frequency f_0. In all of them, significant couplings are observed either between the carrier and its sidebands or between the sidebands alone.

In Figure 6, the most significant interaction is marked by an arrow and corresponds to a resonance of the type $1.48 + 1.90 = 1.69 + 1.69$ Hz. These frequencies correspond to two sidebands plus a self-interaction of the carrier. We must stress that this interaction involves four waves and that it cannot be easily reduced to a three-wave resonance of the type $1.48 + 1.90 = 3.38$ Hz. Given the significant value of the tricoherence, we have evidence here for a cubic nonlinearity. Such four-wave interactions are known to lead to modulational instabilities. Why this nonlinearity disappears in the presence of wind remains an open question, although it is likely to be due to a stabilizing effect of the wind on the modulational instability.

5 Discussion

In which follows, we shall recall some of the above results and discuss about their possible impacts on the understanding of the wavefields evolution.

For the wind generated wavefield, the lack of evidence for a saturation of the correlation integral function suggests a dimension larger than, say, 4, or an infinite dimension. In the latter case, the field would behave like a narrow-band random noise. This appears hardly possible in view of the fact that there exists clear phase locking among the Fourier components close to the peak frequency as shown by the bicoherence function. Such phase locking would confirm previous observations (Ramamonjiarisoa and Mollo-Christensen, 1979; Lake and al, 1977) that wind generated wavefields in laboratory facilities on deep water are much less dispersive than expected by water wave theory. These observations yielded to propose that such fields are dominated by a Stokes-like component suffering the effects of resonant wave-wave interactions. However, as shown by the tricoherence function, no significant cubic interactions seem to be present (see Figure 6.i). Then, it remains the case of large, but not infinite dimension. This would be related with the presence of competitive deterministic and random features of the fields whose correct mathematical and physical formulation has to be found. As far as the spectral evolution is concerned, a similarity-like approach such that of Deardorff (1967) appears quite appropriate.

Also, for the pure mechanical waves, no saturation of the correlation integral function is observed. But as already said in section 4.4, the existence of a finite dimension is not excluded. If such dimension exists, then it is certainly smaller than that of pure wind waves. A striking difference with the latter case is the presence of interactions between the fundamental component at frequency $f_0 = 1.69Hz$ and the sideband components at frequencies $f_\pm = 1.69 \pm 0.2Hz$ as clearly shown by tricoherence function. Recalling that the order value of the wave steepness is 0.2, the condition required for a Benjamin-Feir instability (Benjamin and Feir 1967) is well satisfied. Note however that, strictly speaking, the actual stage of evolution of the observed wavefield would be beyond the domain of such instability theory which is linear and, in addition, which predicts a symmetrical development of the sidebands energy. These facts suggest that the observed field of pure mechanical wave is dominated by a cubic wave resonant interactions process. According to recent advances on the interaction processes, the asymmetry could be associated with dissipation by viscosity and/or breaking waves (Lake et al, 1977; Trulsen and Dysthe, 1990; Tulin and Waseda, 1999). But higher order effect (Dysthe,1979) and multi-wave interactions (Krasitskii, 1994; Krasitskii and Kalmykov, 1993) may be involved as well. The detailed examination of this observed asymmetry, accounting especially for these recent analyses, is behound the scope of this work.

Despite the small value of the correlation dimension, the dynamics involved in the evolution of the mixed wavefield appears the most difficult to understand. The bicoherence function shows high phase locking between the fundamental mode and the other modes present in the spectrum in addition to the higher harmonics. This means that the wind generated modes propagate also at the velocity of the fundamental, mechanically generated mode. As a result, the field is quasi non dispersive. This is not in contradiction with the small value of the correlation dimension mentioned previously. This would also agree with the phase portrait which is reminiscent of that of a process with a limit cycle. The tricoherence function shows no evidence of efficient modal resonant interactions. We believe that, in this case, the dynamics is dominated by the flow interactions between the wind and the waves rather the intrinsic nonlinearity of the wavefield. The interactions would have two effects: i.) the amplification of the wavefield which reach a stable quasi-periodic state; ii.) the annihilation of resonant modal interactions because of the presence of the wind wave components (Alber,1978).

6 Conclusions

Considerable progress has been made in the development of concepts and techniques in the field of the so-called nonlinear dynamical systems with applications to various physical systems (see e.g. Tsonis, 1992). Surprisingly, there are few applications only to water surface waves despite the fact that their dynamics are intrinsically nonlinear.

This work is concerned with applications to laboratory water surface wave fields for which evidence of nonlinear

behaviour has been shown by various authors through extensive use of the harmonic analysis. Of particular interest is the lack of dispersion observed in wind generated waves (see e.g. Ramamonjiarisoa and Coantic, 1976; Ramamonjiarisoa and Mollo-Christensen, 1979). The lack of dispersion has been attributed to the generation of higher harmonics of the so-called dominant component in the spectrum. This quite naturally yielded to try to model this dominant component in terms of Stokes-like waveform (see Lake and Yuen, 1978). As consequence, it has been often suggested that much of the laboratory wavefields are dynamically dominated by such waveform. Surprisingly, our results concerning three typical fields do not confirm this statement. Rather, the evolution of the fields appear to be dominated by distinct physical processes as proposed in the previous section.

We found the use of the concepts and the techniques of nonlinear dynamic system to be of main interest in comparing various fields to identify some eventual common behaviour. On the other hand, in considering a particular field, the corresponding quantities (correlation dimension, optimum time lags,...) are for the moment difficult to express in terms of simple physics and much have to be done in that respect. Example of such difficulty can be found in Mayer-Kress and Elgar (1989).

A prospective task concerns the applications to field experiments in order to compare with the actual results. One specific question of current interest concerns the strength of the nonlinearity involved in both type (laboratory and field) of observations.

Acknowledgements. The authors thank V. Shrira for insightful discussions and his continuous interest in the research project, P. Legal and H. Branger for making comments on the manuscript and K. Dysthe for his helpful discussion about the revised version.

References

Abarbanel, H. D. I., Analysis of observed chaotic data, *Springer, Berlin*, 1996.

Alber, I.E., The effects of randomness on the stability of two-dimensional surface wavetrains. *Proceedings of the Royal Society of London , seria A 363*, 525, 1978

Benjamin, T.B., and Feir, J.E., The desintegration of wave trains in deep water. Part 1. Theory. *Journal of Fluid Mechanics, 27*, 417, 1967

Benney, D. J., Nonlinear gravity wave interactions *Journal of Fluid Mechanics, 14*, 577, 1962

Buzug, Th., Stamm, J., and Pfister, G., Fractal dimensions of strange attractors obtained from the Taylor-Couette experiments, *Physica A, 191*, 559, 1992

Coantic, M., and Favre, A., Activities and preliminary results of air-sea interaction research at IMST, *Adv. Geophys., 16*, 391, 1974.

Deardorff, J. W., Aerodynamic theory for wave growth, with constant wave steepness *Proc. Oceanographical Soc. Japan, 23*, 278, 1967.

Dysthe, K. B., Note on a modification to the nonlinear Schrödinger equation for application to deep water waves, *Proc. Roy. Soc. London A, 369*, 105, 1979.

Eckmann, J.-P., and Ruelle, D., Ergodic theory of chaos and strange attractors, *Rev. Mod. Phys., 57*, 617, 1985.

Fraser, A. M., and Swinney H. L., Independent coordinates for strange attractors from mutual information *Phys. Rev. A, 33*, 1134, 1986.

Haykin, S., and Puthusserypady S., Chaotic dynamics of sea clutter, *Chaos, 7*, 777, 1997.

Herzel, H., Berry, D. A., Titze, I. R., and Saleh M., Analysis of vocal disorders with methods from nonlinear dynamics, *J. Speech Hearing Res., 37*, 1008, 1994.

Kantz, H., and Schreiber, T., Nonlinear time series analysis, *Cambridge University Press, Cambridge*, 1997.

Kim, Y. C., and Powers. E. J., Digital bispectral analysis and its applications to nonlinear wave analysis, *IEEE Trans. Plasma Sci., PS-7*, 120, 1979.

Kitaigorodskii, S. A., A general explanation of the quasi-universal form of the spectra of wind generated gravity waves at different stages of their development, *Johns Hopkins API Technical Digest, Vol. 8*, Num. 1, 1987

Krasitskii, V. P., On reduced equations in the Hamiltonian theory of weakly nonlinear surface waves *Journal of Fluid Mechanics, 272*, 1, 1994.

Krasitskii, V. P., and Kalmykov V. A., Four-wave Reduced Equations for Surface Gravity Waves, *Izvestiya, Atmospheric and Oceanic Physics, 29*, 222, 1993.

Kravtchenko-Berejnoi, V., Lefeuvre, F., Krasnosel'skikh, V. V., and Lagoutte, D., On the use of tricoherent analysis to detect non-linear wave-wave interactions, *Signal Proc., 42*, 291, 1995.

Lake, B. M., Yuen, H. C., A new model for nonlinear gravity waves. Part 1. *Journal of Fluid Mechanics, 88*, 33, 1978.

Lake, B. M., Yuen, H. C., Rungaldier, H., and Ferguson, W. E., Nonlinear deep-water waves: theory and experiment. Part2: Evolution of a continuous wave train, *Journal of Fluid Mechanics, 83*, 49, 1977.

Mayer-Kress, G., and Elgar S., Observations of the Fractal Dimension of Deep and Shallow Water Ocean Surface Gravity Waves, *Physica D, 37*, 104, 1989.

Melville, W. K., Wave modulation and breakdown, *Journal of Fluid Mechanics, 128*, 489, 1983

Mendel, J. M., Tutorial in higher order statistics (spectra) in signal processing and system theory: theoretical results and some applications, *Proc. IEEE, 79*, 278, 1991.

Middleton, D., and Mellen, R. H., Wind-Generated Solitons: A potentially Significant Mechanism in Ocean Surface: Wave Generation and Surface Scattering. *IEEE,J. Oceanic Engineering OE-10*, 471, 1985.

Middleton, An Introduction to Statistical Communication Theory, *McGraw Hill, New York*, 1960.

Nam, S. W., and Powers, E. J., Application of higher order spectral analysis to cubically nonlinear system identification, *IEEE Trans. Acoust. Speech Signal Proc., ASSP-42*, 1746, 1994.

Nikias, C.L., Petropulu, A.P., Higher Order Spectra analysis, *TPR Prentice Hall, New Jersey*, 1993.

Ott, E., Sauer, T., and Yorke, J. A., Coping with chaos, *Wiley, New York*, 1994.

Phillips, O. M., The dynamics of the Upper Ocean, 2nd edition, *Cambridge University Press*, 1977.

Ramamonjiarisoa, A., and Mollo-Christensen, E., Modulation characteristics of sea surface waves, *Journal of Geophysical Research, 84*, 7769, 1979.

Ramamonjiarisoa, A., and Coantic, M., Loi expérimentale de dispersion des vagues produites par le vent sur une faible longueur d'action, *C.R. Acad. Sci. Paris B, 282*, 111, 1976.

Ramamonjiarisoa, A., Contribution á l'Etude de la Structure Statistique et de Mécanisme de Génération des Vagues de Vent,

Thèse de Doctorat, Université de Provence, Marseille, 1974.

Ramamonjiarisoa, A., Sur l'évolution des spectres d'énergie des vagues de vent à fetchs courts. *Mémoires Société Royale des Sciences de Lièges, 6, Tome VI*, 47, 1973

Shugan, I., and Voliak, K., On phase kinks, negative frequencies, and other third-order peculiarities of modulated surface waves. *Journal of Fluid Mechanics, 368*, 321, 1998.

Subba Rao, T. and Gabr, M. M., Introduction to bispectral analysis and bilinear time series models, *Lecture notes in statistics, Springer, New York*, 1984.

Summhammer, J., Rauch, H., and Tuppinger, D., Stochastic and deterministic absorption in neutron-interference experiments, *Physical Review A, 36*, 4447, 1987.

Toba, Y., Local Balance in the Air-Sea Boundary Processes: III./ On the Spectrum of Wind Waves, *Journal of the Oceanographical Society of Japan, 29*, 209, 1973

Trulsen, K., and Dysthe K., Frequency down-shift through self modulation and breaking, in *Water Wave Kinematics, Torum A. and Gudmestad (eds.)*, 561, Kluwer Academic Publishers. Netherlands, 1990

Tsonis, A., Chaos: from theory to Applications, *Plenum Press, New York*, 1992.

Tsonis, A., and Elsner, J. B., Multiple attractors, fractal basins and longterm climate dynamics, *Contrib. Atmos. Phys., 63*, 171, 1990.

Theiler, J., Eubank, S., Longtin, A., Galdrakian, B., Farmer, J. D., Testing for nonlinearity in time series: the method of surrogate data, *Physica D, 58*, 77, 1992.

Tullin, M. P., and Waseda T. Laboratory observations of wave group evolution, including breaking effects, *Journal of Fluid Mechanics, 378*, 197, 1999.

Vyshkind, S., Ya., and Rabinovitch, M. I., The phase stochastization mechanism and the structure of wave turbulence in dissipative media, *Sov. Phys JETP, 44*, 292, 1976.

West, B. J., Statistical properties of water waves. Part I. Steady-State distribution of wind-driven gravity-capillary waves, *Journal of Fluid Mechanics, 17*, 187, 1982.

Yuen, H. C.; Lake B. M., Instabilities of waves on deep water, *Ann. Rev. Fluid Mech., 12*, 303, Ann. Review Inc., 1980.

Zakharov, V. E., The instability of waves in nonlinear media, *Sov. Phys JETP, 51*, 1107, 1967.

Zakharov, V. E., Musher, S. L., and Rubenchik, A. M., Hamiltonian approach to the description of non-linear plasma phenomena, *Phys. Rep., 129*, 285, 1985.